The Third-element Effect on the Oxidation of Ni-xCr-7Al Alloys (x = 0, 5, 10 at.%) at 1173K*

X.J. Zhang [1,2], F. Gesmundo [1] and Y. Niu [1,*]

[1] *State Key Laboratory for Corrosion and Protection, Institute of Metal Research, Chinese Academy of Sciences, Wencui Road 62, 110016 Shenyang (China)*

[2] *Shenyang Institute of Chemical Technology, 110142 Shenyang (China)*

(Received September 26, 2005; final form October 1, 2005)

ABSTRACT

The oxidation in 10^5Pa of pure oxygen of three Ni-xCr-7Al alloys (x = 0,5,10 at.%) was studied at 1173K. A dense external scale of NiO overlying a zone of internal oxidation formed on Ni-7Al and Ni-5Cr-7Al. On the contrary, an external Al_2O_3 layer formed on Ni-10Cr-7Al. Thus, the addition of sufficient Cr levels to Ni-7Al produced a classical third-element effect, inducing the transition between the internal and external oxidation of Al. This effect is interpreted on the basis of an extension to ternary alloys of a criterion first proposed by Wagner for the transition between the internal and external oxidation of the most reactive component in binary alloys.

Key words: ternary alloys; Ni-Cr-Al; oxidation; third-element effect

1. INTRODUCTION

For applications in oxygen-rich environments at very high temperatures, alloys and coatings are often designed to develop surface layers of Al_2O_3 /1/. The development of Al_2O_3 scales on Ni-, Fe- and Co- based binary alloys is possible by using sufficiently high Al contents (6-12 mass%) /1-2/. Unfortunately, the Al levels needed to establish alumina scales on binary alloys often result in unacceptable mechanical properties. In practice, adding Cr to Ni-Al alloys reduces the concentration of Al required to establish the Al_2O_3 scale /1,3/. This is an example of a more general phenomenon of considerable practical importance, called the third-element effect (TEE), by which the presence of a third element can reduce the content of the most reactive element needed to form its oxide as an external scale on ternary alloys as compared to binary alloys with the most noble component /1/.

According to an initial suggestion by Wagner /4/, the third element, e.g. Cr in M-Al alloys, acts as a getter for oxygen in the alloy and prevents the internal oxidation of the most reactive component, Al, producing external Al_2O_3 layers at lower Al levels than in binary M-Al alloys. One of the possible mechanisms, recently summarized by Stott *et al.* /1/, attributes this effect to the simultaneous precipitation of the internal oxides of the two most reactive components in ternary alloys. The overall volume fraction of internal oxide produced in this way reaches the critical value required for the transition to their external oxidation, according to a criterion defined by Wagner /5/, under contents of the most reactive component smaller for ternary than for binary alloys. A semi-quantitative treatment based on this assumption, developed recently /6/, is applied here to the oxidation at 1173K of the present Ni-Cr-Al alloys.

* Correspondent: yniu@imr.ac.cn (Dr. Y. NIU);
Fax N.: 86-24-23978624

2. EXPERIMENTAL

The actual composition of the three Ni-xCr-7Al alloys (all in at. %, if not specified) is 6.6 Al, 5.0 Cr - 6.8Al and 10.0Cr - 7.3Al, balance Ni. They were prepared from high-purity metals by arc-melting and were subsequently annealed in 10^5Pa Ar at 1373°C for 24 h. Flat specimens were cut from the ingots by a diamond wheel saw, ground down to 1200 SiC paper, washed and dried immediately before use. Oxidation tests were carried out in 10^5Pa of pure O_2 at 1173K for 24 h using a Cahn thermobalance. The scales were characterized by Scanning Electron Microscopy (SEM) and an energy-dispersive X-ray spectrometer (EDS) attached to SEM to establish the nature, composition and spatial distribution of the reaction products.

3. RESULTS

3.1 Oxidation kinetics

The oxidation kinetics of the Ni-xCr-7Al alloys at 1173K in 10^5Pa O_2 are shown in Fig. 1 as parabolic plots. The kinetics of Ni-7Al and Ni-5Cr-7Al obeyed the parabolic rate law to a good approximation for the whole test duration with the rate constants equal to $1.0x10^{-3}$and $5.9x10^{-3}g^2m^{-4}s^{-1}$, respectively. Conversely, the kinetics of Ni-10Cr-7Al presented a transition from a first faster nearly parabolic stage with a rate constant of $2.1x10^{-5}$ $g^2m^{-4}s^{-1}$, lasting for about 3 h, to a second parabolic stage with a reduced rate constant of $9.9x10^{-6}$ $g^2m^{-4}s^{-1}$ from 4 to 24 h.

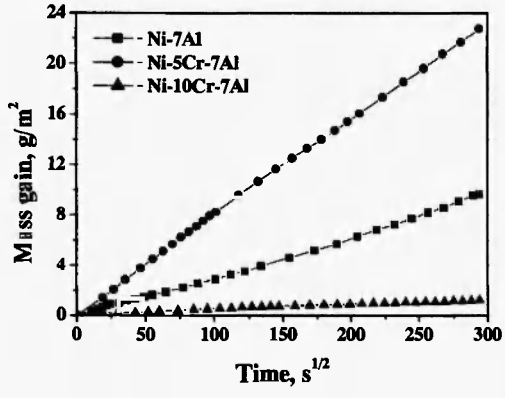

Fig. 1: Kinetics of the Ni-xCr-7Al alloys oxidized at 1173K in 10^5 Pa O_2 for 24 h.

3.2 Scale morphology and microstructure

The microstructure of the scales formed on the three alloys after 24 h oxidation at 1173K in 10^5Pa O_2 is shown in Fig. 2. Ni-7Al (Fig.2a) formed a dense external layer of NiO containing some Ni-Al spinel particles in an inner region corresponding to the alloy consumption zone, followed by a zone of internal oxidation of Al. The scale formed on Ni-5Cr-7Al (Fig.2b) is composed of an outer layer of NiO containing about 1 % Cr and 2 % Al, followed by a region of internal oxidation of both Al and Cr. Finally, an exclusive and continuous external layer of Al_2O_3 formed by oxidation of Ni-10Cr-7Al at 1173K (Fig. 2c).

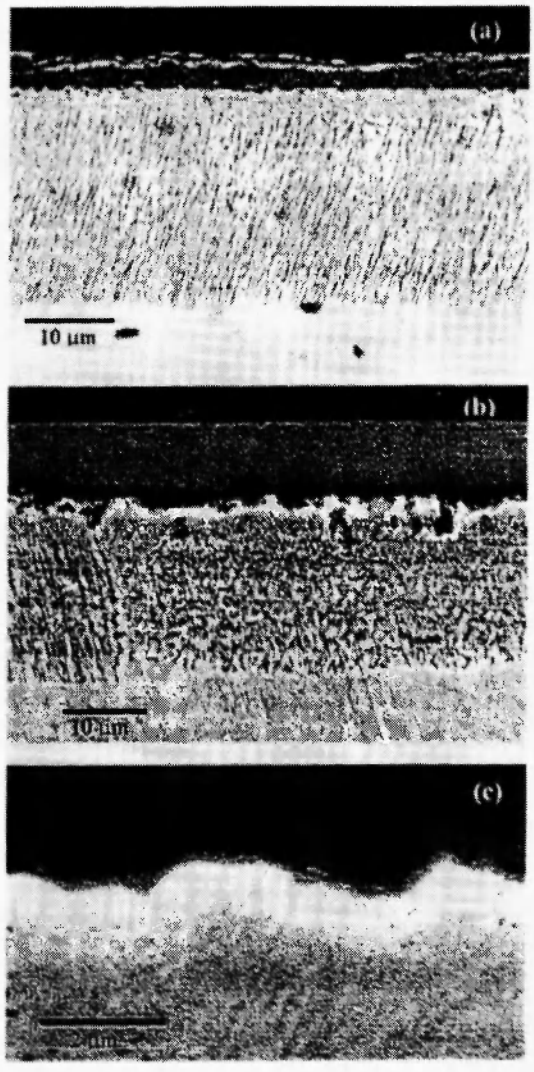

Fig. 2: Cross sections (SEM/BEI) of Ni-7Al (a), Ni-5Cr-7Al (b) Ni-10Cr-7Al (c) oxidized for 24h at 1173K in 10^5Pa O_2.

4. DISCUSSION

4.1 Previous studies of the oxidation of Ni-Al, Ni-Cr and Ni-Cr-Al alloys

An extensive investigation of the oxidation of binary Ni-Al alloys was carried out by Pettit at 1173-1573K in 10^4Pa O_2 /7/. At 1273K the minimum Al content needed to avoid the internal oxidation of Al is of about 8 mass% (15.9 at.%), while the Al content needed to form an exclusive Al_2O_3 scale is of about 17 mass% (30.8 at.%). According to Wood and Stott /2/ the critical Al content needed to form stable protective alumina on binary Ni-Al alloys at 1273K ranges from 7 to 12.5 mass% Al. According to Giggins and Pettit /8/, the critical Cr content needed to avoid the internal oxidation is of about 10 mass% at 1073-1273K, while that required to form exclusive external chromia scales is of about 30 mass% at 1073-1173K, but of only 20 mass% at 1273-1473K /8/.

The oxide maps concerning the oxidation of Ni-Cr-Al alloys at 1273-1473K established by Giggins and Pettit /3/ contain three regions with different oxidation mechanisms. The first region (I) includes alloys forming an external NiO scale overlying a zone of internal oxidation, the second (II) alloys forming an external Cr_2O_3 layer over an Al_2O_3 subscale and finally the third (III) alloys forming a continuous external layer of Al_2O_3. It was further concluded that the presence of Cr was able to reduce the Al content needed to form external Al_2O_3 scales with respect to binary Ni-Al alloys /3/. The present paper examines the possibility that the mechanism of this beneficial effect of Cr additions is based on a synergism between the simultaneous internal precipitation of Cr plus Al.

4.2 Oxidation of ternary Ni-Cr-Al alloys

The exclusive growth of external Al_2O_3 scales in the oxidation of ternary Ni-Cr-Al alloys requires avoidance of two different kinds of internal oxidation: 1) the coupled internal oxidation of Al and Cr beneath external NiO scales and 2) the internal oxidation of Al beneath external chromia scales. The critical Al contents needed for the transitions from these forms of internal oxidation to the external oxidation of Al are calculated separately below.

4.2.1 Transition 1 - The transition between the coupled internal oxidation of Cr plus Al beneath external NiO scales and their external oxidation in ternary Ni-Cr-Al alloys

The calculation of the critical Al and Cr contents needed to prevent their coupled internal oxidation beneath external NiO scales, $N_{Cr}^{o*}(t)$ and $N_{Al}^{o*}(t)$, may be carried out using a recent extension to ternary alloys /6/ of the criterion defined by Wagner /5/. This calculation requires the solution of a system of two equations. Considering the general case of A-B-C alloys where A, B and C form the oxides AO, BO_ν and CO_μ, respectively, and assuming that the oxides of B and C precipitate at the same front of internal oxidation, one of the equations, concerning the kinetics of this process, has the form /6/

$$N_O^{so} = G(\gamma)\,[\,\nu\, N_B^o/F(h_B) + \mu\, N_C^o/F(h_C)]\,[\mathrm{erf}(\gamma) - \mathrm{erf}(u_O)]/\mathrm{erf}(\gamma) \quad (1)$$

where N_O^{so} is the concentration of oxygen in the matrix of pure A under the oxygen pressure for the equilibrium between A and AO, while γ is a parameter related to the kinetics of internal oxidation through the equation /9/

$$\xi^2 = 4\,\gamma^2\, D_O\, t \quad (2)$$

where ξ is the distance of the front of internal oxidation from the original location of the alloy surface and t is time. Moreover, $h_B = \gamma\varphi_B^{1/2}$ and $h_C = \gamma\varphi_C^{1/2}$ with $\varphi_B = D_O/D_B$ and $\varphi_C = D_O/D_C$, where D_O, D_B and D_C are the diffusion coefficients of O, B and C in the alloy. Finally, u_O is defined as

$$u_O = \tfrac{1}{2}\,[k_c(AO)/D_O]^{1/2} \quad (3)$$

where $k_c(AO)$ is the parabolic rate constant for the growth of AO scales expressed in terms of thickness of metal consumed, while F(r) and G(r) are two auxiliary functions defined as /10/

$$F(r) = \pi^{1/2}\, r\, \exp(r^2)\, \mathrm{erfc}(r) \text{ and } G(r) = \pi^{1/2}\, r\, \exp(r^2)\, \mathrm{erf}(r)$$

The second equation needed to calculate the relation between the critical contents of B and C needed for this transition in ternary alloys, $N_B^{o*}(t)$ and $N_C^{o*}(t)$, has the form /6/

$$f_v^*(ov) = N_B^{o*}(t)\,\rho(BO_v)/F(h_B) + N_C^{o*}(t)\,\rho(CO_\mu)/F(h_C) \quad (4)$$

where $f_v^*(ov)$ is the critical overall volume fraction of the two internal oxides required for the transition, still set equal to 0.3, while $\rho(BO_v)$ and $\rho(CO_\mu)$ are the ratios between the molar volumes of the alloy and BO_v and CO_μ, respectively.

The data needed for this calculation are the solubility of oxygen in Ni, $N_O^{s_o}$(Ni) and the diffusivity of oxygen in nickel, D_O(Ni), given by /11/, the diffusion coefficient of Al in Ni, D_{Al}(Ni-Al), given by /12/ and the diffusion coefficient of Cr in Ni-20Cr alloys, D_{Cr}(Ni), given by /13/. Another parameter required is the parabolic rate constant for the growth of NiO at 1173K, which becomes equal to 1.6×10^{-16} m^2s^{-1} /7/ when expressed in terms of thickness of metal consumed, k_c(NiO). Finally, the molar volume of the alloy is set equal to that of pure Ni (6.59×10^{-6} m^3/mol), while those of alumina and chromia are equal to 1.286 $\times10^{-5}$ and 1.459×10^{-5} m^3 per mole of metal, respectively.

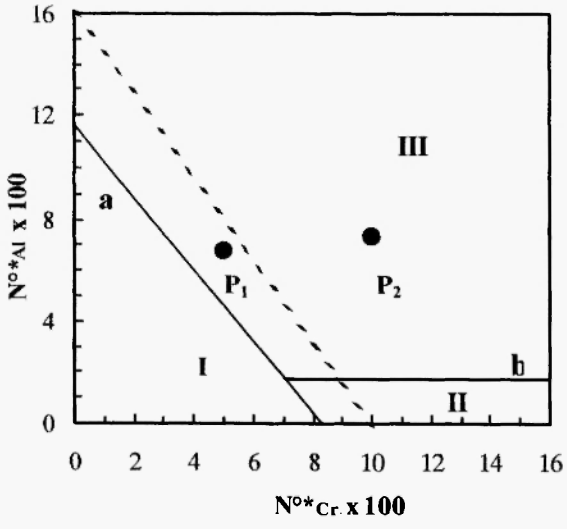

Fig. 3: Critical contents of Cr + Al needed to avoid their coupled internal oxidation beneath external NiO (curve a) and critical Al content needed to avoid its internal oxidation beneath Cr_2O_3 (curve b) for the Ni-Cr-Al system at 1173K. Points P_1-P_2 correspond to the composition of the ternary alloys examined

The system of Eqs.(1) and (2) can be solved for one of the two critical concentrations, e.g. $N_C^{o*}(t)$, using the bulk concentration of the other reactive component [in this case $N_B^{o*}(t)$] as an independent variable, which is allowed to change between zero and the critical value typical for binary A-B alloys. In this approximate treatment ternary diffusion interactions are neglected for simplicity, so that the parameters involved for the ternary alloys have the same values as in the corresponding binary systems. Use of this procedure and of the values of the parameters reported above yields an almost linear relation between the critical content of Al and Cr needed for this transition, $N_{Al}^{o*}(t)$ and $N_{Cr}^{o*}(t)$, as shown by curve a in Fig. 3. Thus, an increase of the Cr content of ternary Ni-Cr-Al alloys produces an almost linear decrease of the corresponding critical Al content. In addition, the same treatment provides also the critical Cr and Al contents needed for the same transition for binary Ni-Cr and Ni-Al alloys, N_{Cr}^{o*}(Ni-Cr) and N_{Al}^{o*}(Ni-Al), which become equal to 8.32 and 11.63 %, respectively. The critical Al content calculated in this way for binary Ni-Al alloys is significantly smaller than the experimental value reported above (15.9%), while the corresponding critical Cr content is rather close to the experimental value (10%). Very likely, the discrepancy between the experimental and calculated values of N_{Al}^{o*}(Ni-Al) depends on the fact that the internal alumina precipitates in Ni-Al alloys have the shape of long rods perpendicular to the alloy surface rather than forming the usual kind of isolated round particles, making the transition to the growth of alumina scales more difficult /14/. The dashed line in Fig. 3 connects the critical Al and Cr contents measured experimentally for the same transition.

4.2.2 Transition 2 - The transition between the internal oxidation of Al beneath external chromia scales and the growth of external alumina scales

The conditions for the transition considered above (transition 1) are not sufficient to ensure the formation of external alumina scales. In fact, in agreement with the experimental results, the addition of sufficient levels of Cr to Ni-Al alloys with a low Al content does not result in the growth of external alumina scales, but rather in the internal oxidation of Al beneath external

chromia scales, so that, according to the definition by Giggins and Pettit /3/, it produces a transition from region I to region II of the oxide map (transition 2). Thus, the Al level needed for the formation of external alumina scales must also exceed a minimum value needed for this transition, $N_{Al}^{\circ *}(Cr_2O_3)$, which can again be predicted by calculating the borderline between regions II and III of the oxide map.

According to a procedure described in a recent analysis of this problem, one of the equations needed to calculate $N_{Al}^{\circ *}(Cr_2O_3)$ is /15/

$$N_{Al}^{\circ *}(Cr_2O_3) = f_v^* F(h_{Al})/\rho(AlO_{1.5}) \quad (5)$$

where h_{Al} is equal to $\Gamma\varphi_{Al}$, with $\varphi_{Al} = D_O/D_{Al}$ and Γ is the kinetic parameter for internal oxidation defined by Eq.(2) as applied to the present case. Another equation involved, concerning the kinetics of internal oxidation, is /15/

$$N_O^s = 1.5\, N_{Al}^{\circ}\, G(\Gamma)\, [erf(\Gamma) - erf(U_O)]/[F(h_{Al})\, erf(\Gamma)] \quad (6)$$

where $U_O = \frac{1}{2}\, [k_c(Cr_2O_3)/D_O]^{1/2}$ and $k_c(Cr_2O_3)$ is the parabolic rate constant for the growth of chromia scales.

An important factor for this calculation is the concentration of oxygen dissolved in the Ni-Cr matrix at the alloy/Cr_2O_3 interface, N_O^s, which will generally differ from the value for the Ni/NiO equilibrium, N_O^{so}, already reported above, because it corresponds to the oxygen pressure for the alloy/Cr_2O_3 equilibrium and thus depends on the activity of Cr at the alloy/scale interface. In particular, N_O^s can be calculated from the known value of N_O^{so} using Sievert's law in the form /16/

$$N_O^s = N_O^{so}\, [P(O_2)^I/P(O_2)(Ni/NiO)]^{1/2} \quad (7)$$

where $P(O_2)^I$ is the oxygen pressure for the alloy/Cr_2O_3 equilibrium and $P(O_2)(Ni/NiO)$ is the corresponding value for the Ni/NiO equilibrium. More precisely, $P(O_2)^I$ is a function of the Cr content in the alloy at the interface with the external chromia scale, N_{Cr}^I, assumed for simplicity to represent also the activity of Cr, which in turn depends on the bulk Cr content of the alloy, N_{Cr}°, as well as on the rate constant for the growth of chromia scales on the alloy through the equation /17/

$$N_{Cr}^I = [N_{Cr}^{\circ} - F(U)]/[1 - F(U)] \quad (8)$$

where $U = \frac{1}{2}\, [k_c(Cr_2O_3)/D_{Cr}]^{1/2}$

A final equation involved concerns the relation between the rate constant for the growth of chromia scales and the Cr content at the alloy-scale interface: this dependence is neglected here for simplicity and also because it is not well known, so that $k_c(Cr_2O_3)$ is simply taken as a constant under constant temperature. In particular, according to the results by Giggins and Pettit on the oxidation of binary Ni-Cr alloys /13/, $k_c(Cr_2O_3)$ at 1173K is equal to 1.3×10^{-17} $m^2 s^{-1}$. Finally, the possible effect of the presence of Cr in the Ni-Cr matrix of the zone of internal oxidation on the solubility of oxygen in the alloy /18/ is also neglected. Solution of the system of Eqs.(5-6) with the help of Eqs.(7-8) using the above values of the various parameters yields $N_{Al}^{\circ *}(Cr_2O_3)$ as a function of N_{Cr}°, shown as curve b in Fig. 3. In the range of composition considered $N_{Al}^{\circ *}(Cr_2O_3)$ is practically constant and equal to about 1.7 % Al. In Fig. 3 curve b is actually interrupted at its crossing point with curve a, corresponding to $N_{Cr}^{\circ *} \cong$ 7.1 %, because in region I curve b is only virtual. The value of $N_{Al}^{\circ *}(Cr_2O_3)$ calculated above (1.7 %) is much smaller than that calculated above for binary Ni-Al alloys (11.63%): this is a consequence of both the low values of N_O^s prevailing under external chromia scales as compared to N_O^{so} and of the lower value of $k_c(Cr_2O_3)$ as compared to $k_c(NiO)$. In fact, if $N_{Al}^{\circ *}(Cr_2O_3)$ is calculated using the correct value of $k_c(Cr_2O_3)$, but setting $N_O^s = N_O^{so}$, the value of $N_{Al}^{\circ *}(Cr_2O_3)$ around the point of crossing with curve a becomes equal to about 8.3%. Conversely, if $N_{Al}^{\circ *}(Cr_2O_3)$ is calculated using the correct N_O^s beneath chromia scales, but setting $k_c(Cr_2O_3) = k_c(NiO)$ it becomes equal to about 5.1%. In any case, according to the previous calculation, to produce external alumina scales on ternary Ni-Cr-Al alloys at 1173K the mole fraction of Al must exceed about 1.7 %.

4.3 Final considerations

The combination of curves a and b divides the plot of Fig. 3 into three fields, which represent the regions of stability of the coupled internal oxidation of Al+Cr beneath external NiO scales (region I, to the left of

curve a). of the internal oxidation of Al beneath external Cr_2O_3 scales (region II, to the right of curve a and below curve b) and finally of growth of external alumina scales (region III, to the right of curve a and above curve b). The two ternary alloys examined, represented by points P_1 and P_2 in Fig. 3, have an Al content largely above that of curve b. Moreover, they both lie to the right of curve a and thus fall in the region of stability of external alumina scales, even though the alloy with 5% Cr is rather close to curve a. However, if the ending points of curve a on the Ni-Al and Ni-Cr sides are displaced at the experimental values of $N_{Al}^{\circ} \cong 15.9$ % and $N_{Cr}^{\circ} \cong 10$ %, the alloy with 5%Cr falls definitely to the left of curve a, corresponding to a coupled internal oxidation of Cr+Al, as observed experimentally. Thus, the oxidation behavior of the present alloys is in substantial agreement with the present model of the transition from the internal to the external oxidation of Cr and Al based on the extension to ternary alloys of the criterion proposed by Wagner for binary alloys.

5. CONCLUSIONS

A binary Ni-7Al alloy and a ternary Ni-5Cr-7Al alloy exposed to 10^5Pa O_2 at 1173K formed external NiO scales followed by a zone of internal oxidation of Al and of Al plus Cr, respectively. Conversely, a ternary alloy containing 7%Al and 10%Cr formed external scales composed of an outer layer rich in Cr and an inner layer rich in Al, while the internal oxidation was suppressed. Thus, a Cr addition ranging between 5 and 10% to Ni-7Al is sufficient to prevent the internal oxidation of Al and to induce the formation of external alumina scales, providing an example of third-element effect. A calculation of the critical Al content needed to avoid its internal oxidation and to form external alumina scales on ternary Ni-Cr-Al alloys, carried out by using an extension to ternary alloys of the criterion proposed by Wagner for the same transition in binary alloys, based on the attainment of a critical value of the overall volume fraction of internal oxides of Cr and Al, is in substantial agreement with the oxidation behavior observed for these alloys.

ACKNOWLEDGMENTS

Financial support by the NSFC under the grant No.50271079 is gratefully acknowledged.

*The paper was presented at the 16th International Corrosion Conference in Sep. 2005 at Beijing, China.

REFERENCES

1. F.H. Stott, G.C. Wood and J. Stringer, *Oxid. Met.*, **44**, 113 (1995).
2. G. C. Wood and F. H. Stott, *Br. Corros. J.*, **6**, 247 (1971).
3. C.S. Giggins and F.S. Pettit, *J. Electrochem. Soc.*, **118**, 1782 (1971).
4. C. Wagner, *Corros. Sci.*, **5**, 751 (1965).
5. C. Wagner, *Z. Elektrochem.*, **63**, 772 (1959).
6. Y. Niu and F. Gesmundo, *Oxid. Met.*, submitted for publication.
7. F. S. Pettit, *Trans. Metall. Soc. AIME.*, **239**, 1296 (1967)
8. C.S. Giggins and F.S. Pettit, *Trans. Met. Soc. AIME*, **245**, 2495 (1969).
9. R.A. Rapp, *Corrosion*, **21**, 382 (1965).
10. J. Crank, *The Mathematics of Diffusion*, Oxford University Press, New York, 1994.
11. J.W. Park and C.J. Altstetter, *Met. Trans.*, **18A**, 43 (1987).
12. W. Gust, M.B. Hintz, A. Lodding, H. Odelius and B. Predel, *Phys. Stat. Sol.*, **64**, 187 (1981).
13. M.S. Seltzer and B.A.Wilcox, *Met. Trans.*, **3**, 2357 (1972)
14. A. Martinez-Villafane, F.H. Stott, J.C. Chacon-Nava and G.C. Wood, *Oxid. Met.*, **57**, 267 (2002).
15. Y. Niu and F. Gesmundo, *Oxid. Met.*, **62**, 391 (2004).
16. 16.D.R. Gaskell, *Introduction to Thermodynamics of Materials*, Taylor and Francis, Washington, 1995.
17. F. Gesmundo and Y. Niu, *Oxid. Met.*, **50**, 1 (1998.)
18. F. Gesmundo and Y. Niu, *Oxid. Met.*, **60**, 347 (2003).